https://doi.org/10.15302/frontphys.2025.064202

RESEARCH RTICLE

Tunable oxygen vacancy defects for high-performance electrolyte-gated synaptic transistors

Qi Chen[1*], Liren Wu[1*], Jiaqi Xu[1], Shuwen Xin[1], Dalong Ge[1], Mengyao Wei[1], Yuanbin Qin[3], Zhen Liu[1], Yan Xi[1, †], Fengyun Wang[1,2, ‡]

[1] College of Physics, Qingdao University, Qingdao 266071, China

[2] State Key Laboratory of Structural Chemistry, Fujian Institute of Research on the Structure of Matter, Chinese Academy of Sciences, Fuzhou 350002, China

[3] School of Materials Science and Engineering, Xi'an Jiaotong University, Xi'an 710000, China

Corresponding authors. E-mail: ‡fywang@qdu.edu.cn, †xiyan@qdu.edu.cn

Received February 2, 2025; accepted April 20, 2025

Supporting Information

Experimental section

Material synthesis

0.038 g of indium nitrate (In $(NO_3)_3$•xH_2O, 99.9%, Aladdin), 0.112 g of zinc nitrate (Zn $(NO_3)_2$•6H_2O, 99.9%, Aladdin) and 0.8 g polyvinyl pyrrolidone (PVP, 1,300,000 g mol^{-1}) were dissolved in 5 ml of N, N-dimethylformamide (DMF, 99.9%, Aladdin) to obtain a homogeneous and transparent InZnO precursor solution. Lithium perchlorate ($LiCLO_4$, Aladdin) was mixed with polyethylene oxide (PEO, Aladdin) in a mass ratio of 8:1. The mixture was then dissolved in 5 mL of acetonitrile (CH_3CH, 99.9%, Aladdin) and stirred for 12 h at room temperature.

Device Fabrication

The Si/SiO_2 substrates were ultrasonic cleaned in deionized water, acetone, and ethanol sequentially, and then thoroughly blown dry with nitrogen. InZnO nanowires were prepared by the electrospinning machine at a DC voltage of 16.5 kV in a flow rate of 0.006 ml min^{-1} and subsequently collected by the substrates. Then, the InZnO nanowires were heated at 150 °C for 10 mins and treated with ultraviolet (UV) irradiation (1 kW, 290-320 nm) for 40 mins, which was advantageous to enhance the adhesion of the nanowires to the substrate. In order to completely remove the organic residues, InZnO nanowires were annealed at 500 °C for 2 h. The Aluminum (Al) source and drain electrodes with a thickness of 90 nm were evaporated by thermal evaporation, and the channel width and length) of the shadow mask was 1000*100) μm. Additionally, in order to investigate the impact of plasma treatment time on the electrical properties of InZnO nanowires, we placed three devices in a Sat-12D plasma cleaner, using ultra-pure Ar as the treatment gas, and the bombardment treatments for the three devices was set as 15, 30 and 45 s respectively. The flow rate of Ar gas was maintained constant at 35 standard cubic centimeters per min, and the power was set as 50 W. After the plasma treatment, 50 μL of ionic liquid was cast onto the channel region to cover the InZnO nanowires.

Material and device characterization

The lattice structure of InZnO nanowires were investigated by XRD (Rigaku D/max-rB). The chemical compositions of nanowires were analyzed by XPS (Axis Supra+). All the electrical characteristics and synaptic functions of the transistors were analyzed using a Keithley B2912A semiconductor parametric analyzer in the atmosphere at room temperature. The specific device measurement conditions were optimized as follows: with the S/D in contact with two

separate tungsten probes and the gate probe in contact with an ionic liquid electrolyte. The electrical signals were acquired from a Keysight B2912A semiconductor parameter analyzer at room temperature, 45% ambient humidity and dark environment.

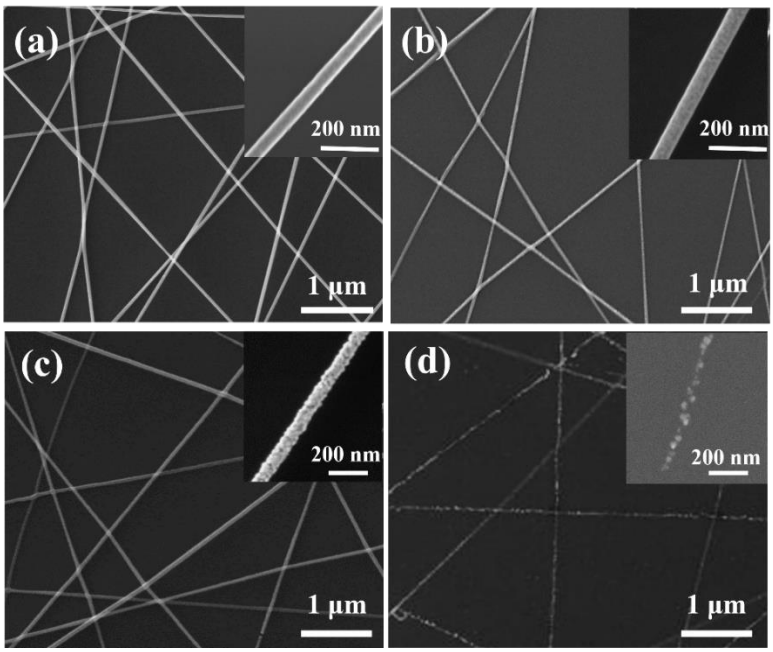

Fig. S1 Scanning electron microscope images with different treatment times. (a) 0 s. (b) 30 s. (c) 100 s. (d) 180 s.

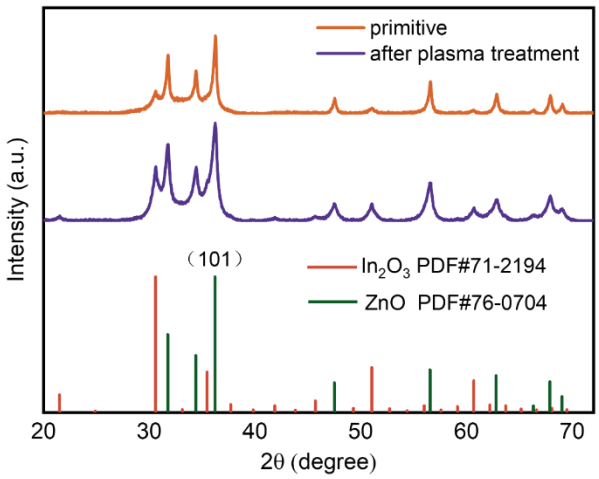

Fig. S2 The XRD patterns of the primitive InZnO nanowires and after 30 s Ar plasma treatment.

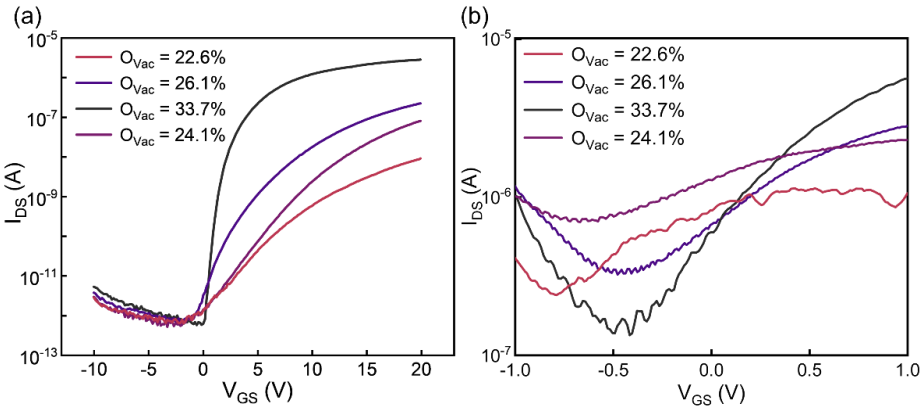

Fig. S3 (a) Transfer curves of InZnO FET (with different oxygen vacancy concentrations) after Ar plasma treatment. (b) Transfer curves of InZnO EGSTs (with different oxygen vacancy concentrations) with $LiClO_4$/PEO electrolytic dielectric.

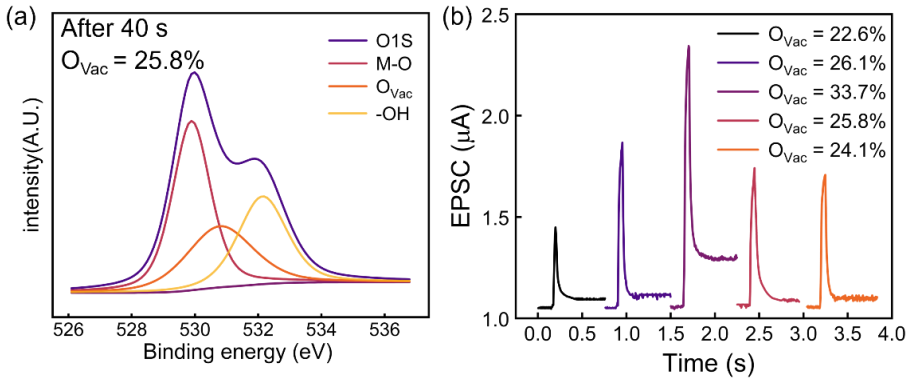

Fig. S4 (a) XPS spectra of InZnO nanowires with 40s Ar plasma treatment time. (b) EPSC of InZnO EGSTs with different concentrations of oxygen vacancy.

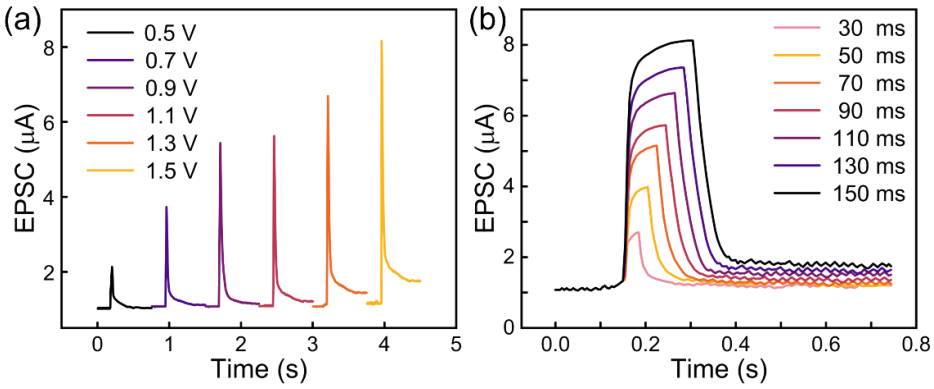

Fig. S5 (a) The dependence of EPSC on the pulse voltage. (b) The dependence of EPSC on the pulse width.

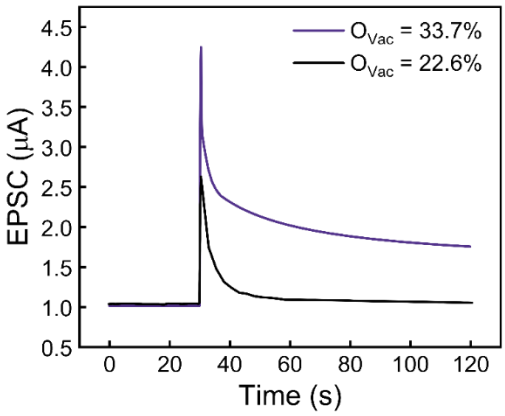

Fig. S6 LTP is triggered by V_{gs} with an amplitude of 1.5 V, pulse width of 30 ms and V_{ds} of 0.5 V.

Table S1 Comparison of EGSTs performance.

No	Electrolyte	Semiconductor	V_{gs} [V]	V_{ds}[V]	PPF(D) Index	Year	[Ref.]
1	ZrOx	ITO	3	0.1	1.65	2020	1
2	–	In_2Se_3	-15	0.2	1.13	2020	2
3	CAAC	IGTO	-5	0.1	1.13	2022	3
4	$LiClO_4$/PEO	InZnO	0.5	0.7	1.38	2022	4
5	Li-AlOx	ZnO/In_2O_3	1	1	1.42	2022	5
6	LiZrO	In_2O_3/ZnO	1.5	1	1.135	2024	6
7	LiPON/LSO	IGZO	-5	5	1.626	2024	7
8	Al_2O_3	In_2O_3	-5	-0.5	1.335	2024	8
9	PEO/LiTFSI/LAGP	P3HT	-5	0.1	1.23	2024	9
10	LiGdO	In_2O_3	4	1	1.46	2025	10
11	[P (VDF-TrFE-CFE)]/chitosan	InZnO	4	1	1.74	2025	11
This work	$LiClO_4$/PEO	InZnO	1	0.5	1.67	2025	This work

References

1. Y. G. Kim, D. Lv, J. Huang, R. N. Bukke, H. Chen, J. Jang, Oxygen vacancies effects in a-IGZO: Formation mechanisms, hysteresis, and negative bias stress effects, Phys. Status Solidi A. 217, 2000314 (2020).

2. B. Tang, B. Tang, S. Hussain, R. Xu, Z. Cheng, J. Liao, Q. Chen, Novel Type of Synaptic Transistors Based on a Ferroelectric Semiconductor Channel, ACS Appl. Mater. Interfaces. 12, 24920(2020).

3. T. Lim, S. Lee, J. Lee, H. Choi, B. Jung, S. Baek, J. Jang, Artificial Synapse Based on Oxygen Vacancy Migration in Ferroelectric-Like C-Axis-Aligned Crystalline InGaSnO Semiconductor Thin-Film Transistors for Highly Integrated Neuromorphic Electronics, Adv. Funct Mater. 33(8), 2212367 (2022).

4. Y. Chang, H. Cong, R. Zhou, W. Zhang, Y. Qin, X. Liu, and F. Wang, Enhanced Artificial Synaptic Properties Enabled

by Arrays of Electrolyte-Gated Electrospun InZnO Nanowires, ACS Appl. Electron. Mater. 4(5), 2570 (2022).
5. Q. Liu, L. Yin, C. Zhao, Z. Wu, J. Wang, X. Yu, Z. Wang, W. Wei, Y. Liu, I. Z. Mitrovic, L. Yang, E. G. Lim, and C. Z. Zhao, All-in-one metal-oxide heterojunction artificial synapses for visual sensory and neuromorphic computing systems, Nano Energy. 97, 107171 (2022).
6. S. Sun, M. Zhang, J. Bian, T. Xu, and J. Su, In_2O_3/ZnO heterojunction thin film transistor for high recognition accuracy neuromorphic computing and optoelectronic artificial synapses, Nanotechnology. 35(36), 365602 (2024).
7. S. K. Kim, S. W. Choi, M. Kim, K. R. Yun, G. Wang, and T. Y. Seong, Dual-Electrolyte Neuromorphic Transistor for Risk Detection and Image Processing, Adv. Mater. Technol. 2401617 (2024).
8. M. Zahid, M. I. Sadiq, C. Jin, J. Wang, X. Shi, W. Liu, F. Aslam, Y. Xu, M. Tahir, J. Yang, and J. Sun, Nitrogen-doped carbon quantum dot-decorated In_2O_3 synaptic transistors for neuromorphic computing, Appl. Phys. Lett. 125(19), 193503 (2024).
9. H. Yu, Y. Xu, Z. Deng, C. Jin, W. Liu, X. Shi, J. Liu, J. Sun, and J. Yang, Self-supported flexible organic electrochemical synaptic transistors on self-healing composite electrolyte membranes, Appl. Phys. Lett. 124(17), 173703 (2024).
10. Y. Du, W. Xiao, G. Miao, Z. Yin, R. Ci, G. Liu, and F. Shan, Solution-processed LiGdO solid electrolyte for an In_2O_3 synaptic transistor and its application in neuromorphic computing, J. Mater. Chem. C (2024).
11. W. Zeng, X. Luo, J. Xu, M. Zhang, S. Liu, Q. Zhang, and G. Zhu, Ferroelectric/Electric-Double-Layer-Modulated Synaptic Thin Film Transistors toward an Artificial Tactile Perception System, ACS Applied Materials & Interfaces (2025).